ISSN 0742-0463, Journal of Volcanology and Seismology, 2013, Vol. 7, No. 2, pp. 112–130. © Pleiades Publishing, Ltd., 2013.
Original Russian Text © T.G. Churikova, B.V. Ivanov, J. Eichelberger, G. Wörner, B. Browne, P. Izbekov, 2013, published in Vulkanologiya i Seismologiya, 2013, No. 2, pp. 27–47.

Major and Trace Element Zoning in Plagioclase from Kizimen Volcano (Kamchatka): Insights into Magma-Chamber Processes

T. G. Churikova[a, b], B. V. Ivanov[a], J. Eichelberger[c], G. Wörner[b], B. Browne[d], and P. Izbekov[e]

[a] *Institute of Volcanology and Seismology, Far East Branch, Russian Academy of Sciences, Piipa bul'var, 9, Petropavlovsk-Kamchatskii, 683006 Russia*
e-mail: tchurikova@mail.ru

[b] *Geochemistry Division, Center of Geological Sciences, Göttingen University, Goldschmidt Str., 1, Göttingen, 37077 Germany*
e-mail: gwoerne@gwdg.de

[c] *Volcanic Hazards Program, USGS, Reston, Virginia, United States*
e-mail: jeichelberger@usgs.gov

[d] *Geological Sciences Department, California State University, Fullerton, California, United States*
e-mail: bbrowne@fullerton.edu

[e] *Volcano Observatory, Geophysical Institute of the University of Alaska, Fairbanks, Alaska, United States*
e-mail: pavel@gi.alaska.edu

Received October, 25, 2010

Abstract—The data on the geochemistry of the rocks of Kizimen Volcano and results of microprobe studies of major and trace elements in plagioclase grains from acid lavas and basalt inclusions are presented. The characteristics of the Kizimen Volcano are the following: (1) basalt inclusions are abundant in acid lavas; (2) banded, mixed lavas occur; (3) the distribution curves of rare-earth elements of acidic lavas and basalt inclusions intersect; (4) Sr–Nd isotope systematics of the rocks and inclusions do not indicate mixture with crustal material; (5) plagioclase phenocrysts are of direct and reverse zonation; (6) olivine and hornblende, as well as acid and mafic plagioclases, coexist in the rocks. The studies revealed that the rocks are of a hybrid nature and originated in the course of repeated mixture of acid and mafic melts either with chemical and thermal interaction of melts or exclusively thermal ones. Study of the major- and trace-element distribution in zonal minerals provides an informative tool for understanding the history of the generation and evolution of melts in a magma chamber.

DOI: 10.1134/S0742046313020024

INTRODUCTION

The processes that occur in magma chambers, such as convection and mixing of magmas, melt differentiation, and growth of crystals in melts, play an important role in magma-rock generation. Experimental and simulated models of these processes, for example [Marsh, 1989], make it possible to study physical parameters, such as density and viscosity, in relation to melt composition, the temperature gradients inside the magma chamber and at its contact with host rock, and chamber geometry. As long as part of the abovementioned parameters may not be uniquely determined in natural systems, the applicability of such models is limited.

The process of magma mixing that was suggested by R. Bunsen in 1851 [Bunsen, 1851] has been actively studied up to recent times; the role of this process in the generation of igneous rocks should not be underestimated. Mixing of partly crystallized magmas most often occurs in island-arc environments where long-existing magma may fractionate up to acid varieties. Here, in addition to cases of magmas with different origins, mixing of magmas of the same origin also occurs. These might separate in the course of differentiation, assimilation, or segregation of magma portions into subsurface chambers [Kawamoto, 1992; Naumov et al., 1997; Couch et al., 2001]. In this case, deeper magmas of mafic (basalt) composition periodically enter into subsurface crustal chambers with acid magma, thus forming a series of hybrid mixed magmas [Ivanov et al., 1978; Eichelberger et al., 1978].

Depending on the degree of mixing, volcanic hybrid lavas may be banded lavas or isolated blocks of basic lava in an acid lava flow, or else relatively uniform lava with phenocrysts that are obviously disequilibrium relative to the groundmass. The process of magma mixing is also noticeable during microscopic examination from the following features: phenocryst resorption and the development of a reaction rim and reverse zonality of minerals due to dissolution of low-temperature minerals as the melt temperature increases and subsequent crystals that are growing from a new hybrid melt, as well as the occurrence of disequilibrium phenocryst associations

[Dungan and Rhodes, 1978; Kadik et al., 1986; Eichelberger et al., 2000, 2006; Plechov et al., 2008].

Currently, many researchers study geochemical zoning in plagioclases, pyroxenes, and other minerals; they consider it as an indicator of the changeability of the mineral-growth environment that allows one to trace the history of mineral crystallization in the rocks of volcanic eruptions. Plagioclases, which frequently involve multilevel zonality, easily respond to changes in magma composition or crystallization conditions [Volynets et al., 1979; Frikh-Khar, 1977; Davidson and Tepley III, 1997; Ginibre et al., 2002a, 2002b]. Major-element zoning in plagioclases, which reflects the diffusion of CaAl–NaSi pairs in the plagioclase An–Ab binary system [Grove et al., 1984; Tsuchiyama, 1985] has been widely used for studying processes in magma chambers. In many simulation models, including [Allegre et al., 1981], attempts have been made to estimate the kinetic aspects of plagioclase crystal growth and resorption.

All these studies assist the understanding of zoning in plagioclases. Nevertheless, up until now the joint influences of several factors, such as temperature, pressure, melt composition, and H_2O content, on the An–Ab system were difficult to recognize.

Due to the development of local high-precision methods of material analysis using electron microprobe and ion probes it became possible to study not only minor elements, which replace major elements in mineral structure and occur at concentrations of 0.1–1.0 wt %, but also trace elements that are usually found in voids of the crystalline lattice of minerals with concentrations below 0.1 wt % [Winter, 2001]. In recent years more papers on the determination of isotope ratios in individual zones of plagioclase crystals have been published. They consider sites several microns in size with the application of ion probe [Brophy et al., 1996] or an isotope mass spectrometer [Churikova and Sokolov, 1993; Davidson and Tepley III, 1997; Tepley III and Davidson, 2000]. These methods significantly expanded the possibilities of identification of various factors that favor plagioclase zoning, including mixing of magmas with different compositions, assimilation, and the influence of temperature. These methods are, however, labor-intensive and expensive; moreover, in the case of ion probe, part of the crystal completely burns out, thus precluding repeated measurements. The present-day electron microprobe allow one to detect several trace elements in concentrations up to 100 ppm in some plagioclase zones on areas a few microns in size [Ginbre et al., 2002a, 2002b]. These instruments can be used to study many samples for both major and trace elements without destruction of the specimens.

In this paper we present the results from an analysis of plagioclase phenocrysts from basalts, andesite–basalts and dacites of Kizimen volcano that were obtained with a modern electron microprobe. Detailed tephra chronological studies [Melekestsev et al., 1992] of the ages of lava flows and the eruptive history of the volcano revealed that it was formed in the Quaternary time and was active during Holocene time (the latest lavas date back to the Late Holocene). At present, active fumarole activity is observed on the slope of the volcano.

The rocks of the volcano were studied in two stages. During the first stage the concentrations of major and trace elements, as well as the isotope ratios of Sr, Nd, and Pb in volcanic rocks, were investigated; at the second stage plagioclase crystals of the most typical samples were studied. An electron microprobe was used for the determination of major (Al, Si, Na, Ca, and K) and trace elements (Ba, Sr, Mg, and Fe) at some sites a few microns in size. The positions of the sites were chosen on high-resolution images in reflected light. Our studies aimed both at investigating the volcano's magmatic evolution and recognizing the processes that influence melt crystallization inside the magma chamber before an eruption.

1. METHODS OF STUDY

All the analytical works were carried out at the Geochemistry Division of the Center of Geological Sciences at Göttingen University, Germany. The concentrations of major elements and some trace elements (Sc, V, Cr, Co, Ni, Zn, Ga, Sr, Zr, and Ba) in the rocks were measured using X-ray fluorescent analysis (XRF). The relative analytical errors ($\pm 2\delta$ for major elements were less than 1% (with the exception of Fe and Na, where the error was 2%) and about 5% for trace elements. The L.O.I. determination error is about 10%. All the other rare elements were measured using the ICPMS method. Errors that were estimated according to the JB3 and JA2 standards equal about 15–20% for Nb and Ta; for other rare elements they are less than 10%.

The Sr, Nd, and Pb isotope ratios were measured using a Finnigan MAT 262 RPQ II+ mass spectrometer using the NBS987 standard (0.710245) for Sr, La Jolla (0.511847) for Nd, and NBS981 (the recommended values according to [Todt et al., 1984]) for Pb. Statistical errors ($\pm 2\sigma$) were less than 0.004% for Sr and Nd and less than 0.1% for Pb. Detailed descriptions of these techniques were given in [Churikova et al., 2001a, 2001b, 2007; Dorendorf et al., 2000a, 2000b].

The concentration of major (Si, Al, Ca, Na, and K) and trace elements (Mg, Fe, Ba, and Sr) in plagioclases were measured by a JEOL8900 WDS electron microprobe using a set of synthetic and natural standards. Some zones in plagioclase crystals were identified on the basis of crystal reflections in back scattered electrons. For clarification of plagioclase evolution during

their growth chemical analyses were performed along profiles from the centers of phenocrysts to their margins; different zones and localities of nonuniformity in the crystals were analyzed. In the same samples the central and marginal parts of microlites were analyzed for comparison.

A technique for the determination of major and trace elements using a JEOL8900 WDS instrument was described in detail in [Ginibre et al., 2002a, 2002]. Quantitative analysis at a point for Al, Si, Na, Ca, K, Ba, Sr, Fe, Ti, and Mg was performed at an accelerating voltage of 20 kV and at a beam current of 40 nA and an area of excitation band from 2 to 5 microns. In the beginning we analyzed alkaline elements and all the major elements (Na, K, Al, Si, and Ca) during the first 90 seconds (the time of measurements at the peak was 16 sec). Minor (Sr and Fe) and trace elements (Ti, Mg, and Ba) were then analyzed for a longer time of up to 4 and 5 minutes at the peak of each element.

2. THE GEOLOGICAL SETTING, PETROGRAPHY, AND MINERALOGY OF THE ROCKS

Kizimen Volcano (height 2485 m; coordinates 55°08.0′ N, 160°19.3′ E) is one of the active Holocene volcanoes of Kamchatka. It is situated at the southeastern flank of the Shchapino graben [Ivanov, 2008], which occurs at the boundary between two active volcanic belts: the Central Kamchatka Depression (CKD) and the Eastern Volcanic Front (EVF). The northwestern part of the volcanic edifice is cut by NE–SW-trending faults and also by a series of ravines in which rocks of the stratovolcano basement outcrop. The only historic eruption is known from reports of hunters who noticed fire jets and black smoke in the area of Kizimen in 1928. As no deposits of a similar age are observed at the volcano's base, that eruption seems to have been a weak one.

The volcano is an intricate complex formed by numerous lava flows and extrusive domes (Fig. 1). According to tephra chronological datings, the age of the rocks varies from 12–11 Ka to 1 Ka [Melekestsev et al., 1992].

The products of the eruptions of Kizimen volcano are of andesite and dacite compositions; they form numerous lava flows and a series of extrusive domes that are concentrated near the top of the volcano. Andesite and dacite flows are saturated with syngenetic inclusions of more mafic basalt and basaltic andesite composition (Fig. 2a). For the sake of brevity, below we will call all the inclusions of a more mafic composition (basalts and basaltic andesites) basalts. In the youngest lavas near the volcano's top the amount of such inclusions may reach 35% of the lava-flow volume. Rather often we observe dacite lavas with inclusions of basaltic andesites, which in their turn contain basalt inclusions (Fig. 2b). Banded lavas occur often with bands from a few millimeters to 20–25 cm wide (Fig. 2c).

In terms of mineral phenocrysts, the volcano rocks are middle–coarse-crystalline, and often serial-porphyric. In chemical composition they form a series from basalts to dacites (Fig. 3, Table). The composition of the lavas varies from basaltic andesites to dacites, while dark-colored inclusions are always of mafic composition and are basalts, more rarely basaltic andesites.

One characteristic feature of the rocks is the coexistence of large phenocrysts of plagioclase (up to 2 cm), hornblende, olivine, and orthopyroxene. All the rocks contain hornblende, belong to a moderately potassic calc-alkali series, and form a narrow fractionating trend (Fig. 3a). Both basalts and hosting dacites form the same trends in different discrimination diagrams. It was found that the composition of basalt inclusions in dacites becomes more mafic in younger lavas (Fig. 3a), suggesting an antidromic history of the volcano's evolution. The Kizimen volcano is not only situated between CKD and EVF; as seen from Fig. 3a, the rocks of the volcano are rich in potassium compared to EVF lavas, but are depleted in it compared to CKD rocks; therefore they occupy an intermediate position between fields of figurative points for rocks of the two volcanic belts of Kamchatka.

3. THE GEOCHEMICAL CHARACTERISTICS OF ROCKS

The distribution of minor and trace elements of the volcanic rocks on spider diagrams (Fig. 3b) is typical of an island-arc series with enrichment in large-ion lithophile elements (LILE: K, Cs, U, Ba, Rb, Sr, and Pb) and depletion in high field-strength elements (HFSE: Nb, Ta, Hf, Zn, and Ti) and rare-earth (REE) elements. At the same time andesites and dacites are enriched in LILE and in light rare-earth elements (LREE: La–Sm) and depleted in heavy rare-earth elements (HREE: Eu–Lu) compared to basalts and basaltic andesites from inclusions, forming intersections of element distribution curves on the spider diagrams for acid and mafic rocks(Fig. 3b).

The observed intersection of curves on the spider diagrams might occur due to different sources for mafic and acid rocks. The spider diagrams of rocks that are crystallized from one melt fractionated to different degrees are usually sub-parallel, more acidic varieties that are enriched in all trace elements compared to mafic varieties. This happens during crystallization of olivine, pyroxenes, plagioclase, and spinel (or magnetite). These minerals contain very small amounts of trace elements; therefore these elements remain in the melt and accumulate in its later portions. When hornblende begins to crystallize from the melt, dacite variet-

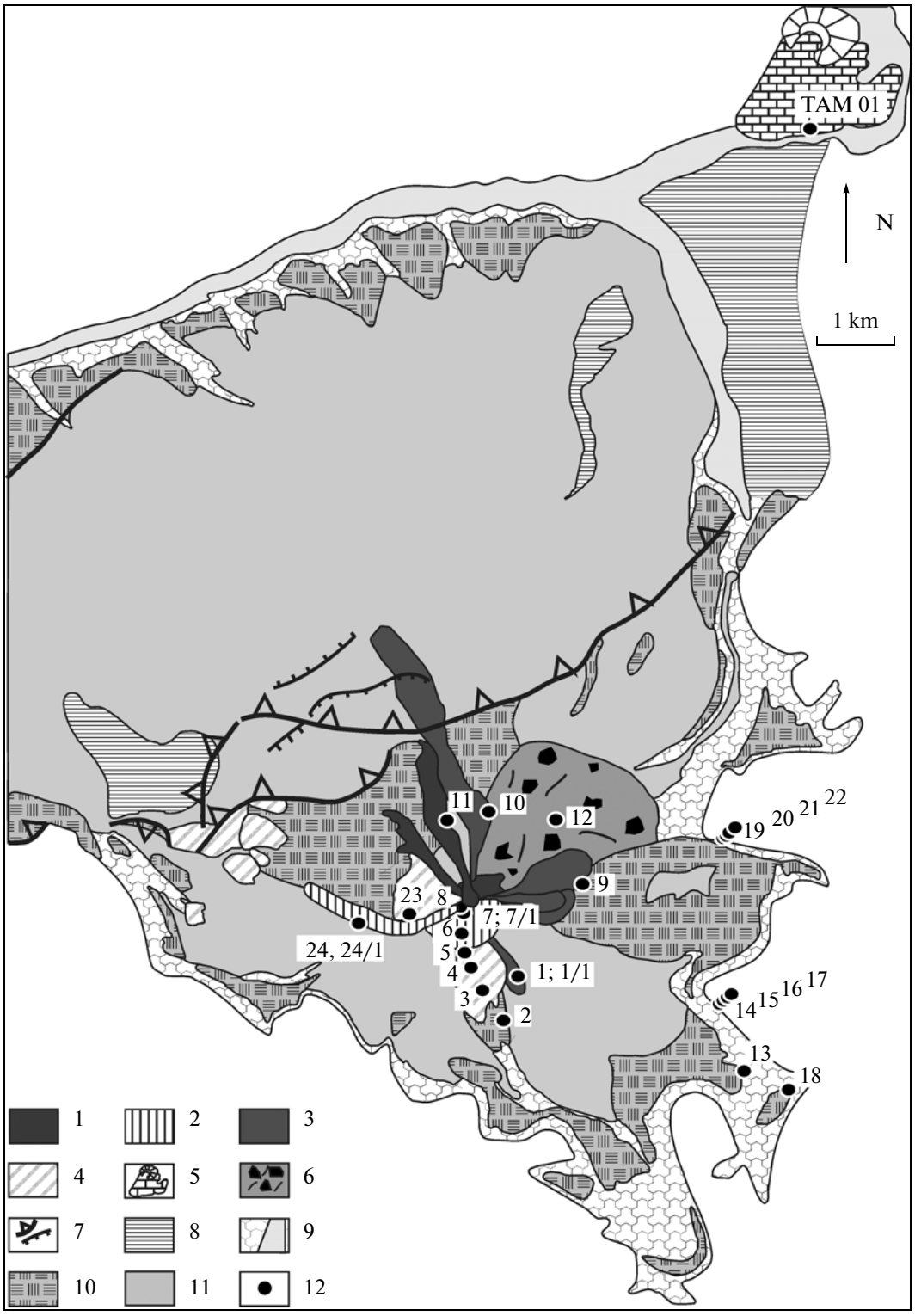

Fig. 1. A sketched map of Kizimen volcano, after [Melekestsev et al., 1992]. Lava flows and extrusive domes: (1) younger than 1100 B.P., (2) 3000–1200 B.P.; (3) lava flows of ages 1200 and 1700 yr; (4) lava flows and extrusive domes of ages 7700 and 11000 yr; (5) Tamara cone of Late Pleistocene age; (6) pyroclastic flows and landslides younger than 3000 yr; (7) faults of different amplitudes; (8) glacial deposits; (9) alluvial deposits; (10) pyroclastic flows and landslides of ages 11 000 and 8400 yr; (11) pyroclastic flows and landslides of ages 8400–3000 yr; (12) sites of geochemical sampling KIZ-96-** and TAM-96-01.

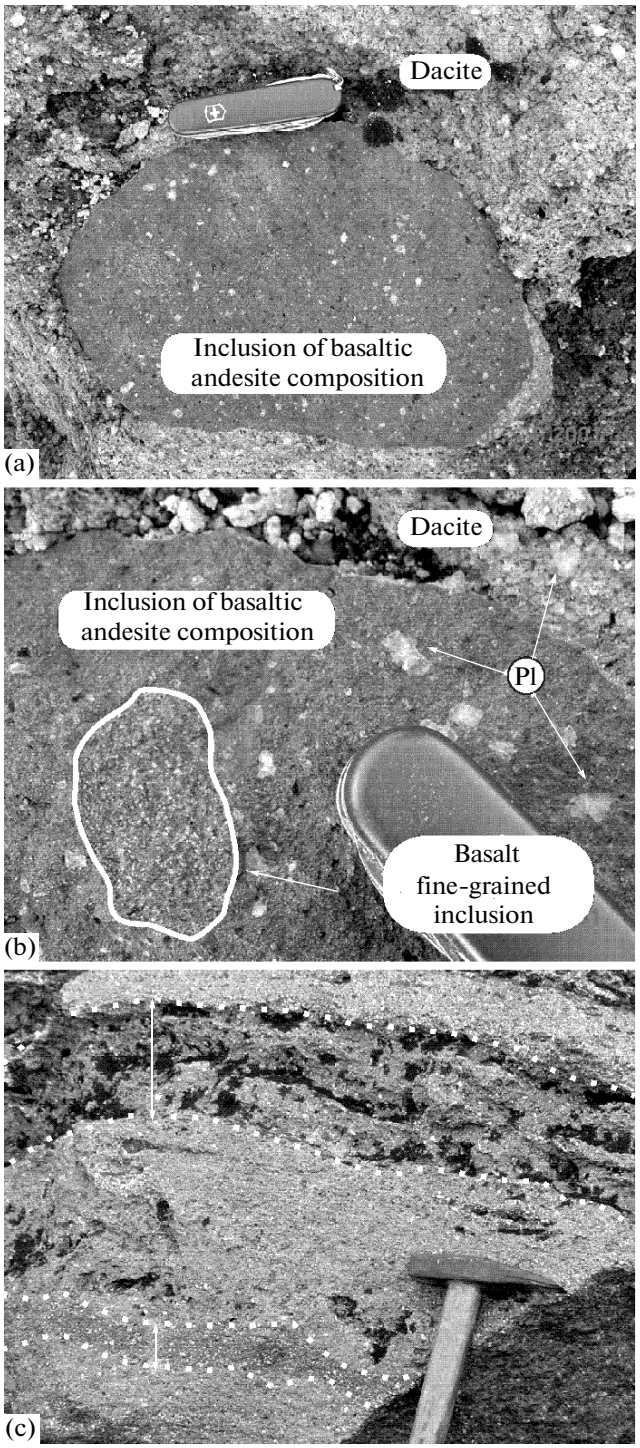

Fig. 2. Lavas of Kizimen Volcano and mafic inclusions in them. A large (17 × 20 cm) basaltic andesite inclusion in dacite lava (a); fine-grained, 3 by 5-cm basalt inclusion (marked with a solid white line) inside the larger basaltic andesite inclusion (b) shown in (a), large plagioclase phenocrysts in basaltic andesite and dacite are marked by arrows; a fragment of banded lava (c), dark strips are highlighted by white dotted lines; their thicknesses are indicated by double arrows.

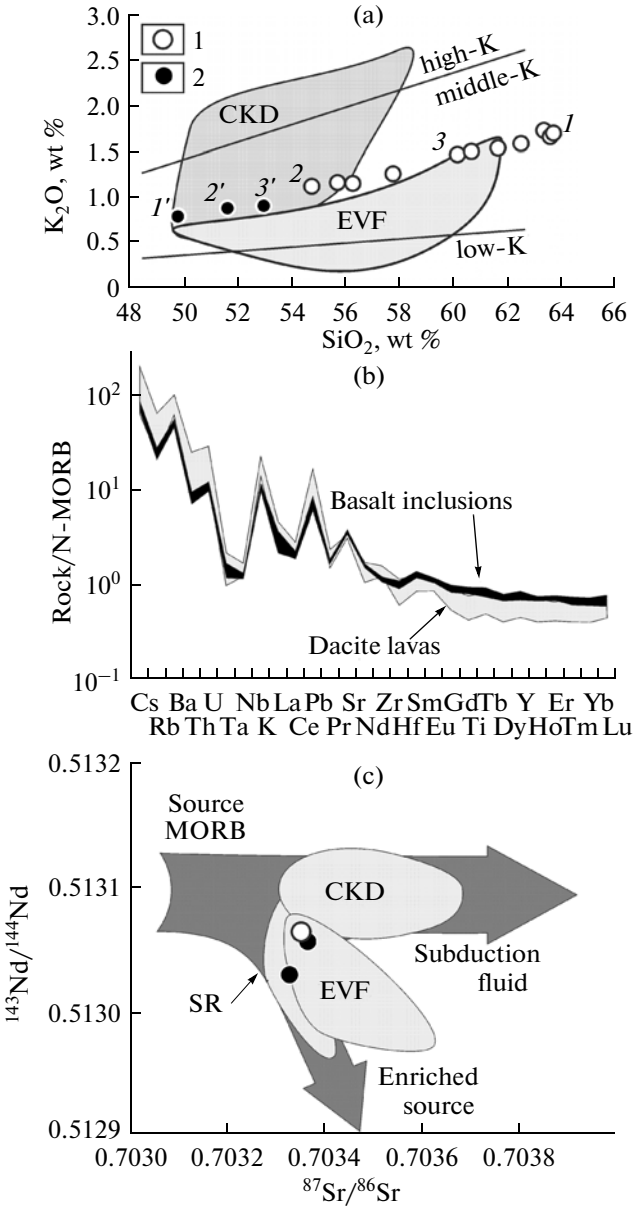

Fig. 3. The geochemical characteristics of the rocks of the Kizimen volcano. (1) Lavas; (2) inclusions of mafic composition in lavas. K_2O–SiO_2 diagram of Kizimen rocks (a). Rocks of EVF and CKD are shown in grey fields using data from [Churikova et al., 2001]. Paired digital symbols (*1–1′*) designate rock pairs (host lava and inclusion, respectively) for three distinct eruptions: *1–1′* for 1600 B.P., *2–2′* for 2700 B.P., *3–3′ f*or 3000 B.P. [Melekestsev et al., 1992].

Diagrams of trace element distributions in rocks of the Kizimen volcano (b): the gray field is the lava of the volcano; the black field is mafic inclusions. The data are normalized to NMORB values after [Sun and McDonough, 1989].

Isotope ratios in rocks of Kizimen Volcano (c). Arrows mark the locations of the three sources of material in Kamchatka rocks: a MORB source, subduction fluid, and an OIB enriched source. Grey shading highlights the fields of EVF, CKD, and SR rocks after [Churikova et al., 2001b; Dorendorf et al., 2000b].

ies are depleted in heavy rare-earth elements and the rare-earth distribution lines of dacite and mafic rocks may intersect. Similar intersections of rare-earth element distribution curves were found and numerically simulated by F. Dorendorf et al. [2000a] for the rocks of Bakening Volcano. Based on these data, we conclude that the intersection of trace-element distribution curves on the spider diagrams of the rocks of Kizimen volcano resulted from an active crystallization of amphibole; this indicates that both basalt inclusions and hosting dacites were formed from either one mantle melt or several that were similar in composition. The active crystallization of amphibole is supported by the fact that all the volcanic rocks, i.e., acid host rocks and mafic inclusions, systematically contain hornblende.

According to the petrographic and geochemical characteristics of rocks (Fo_{72-78}, low Mg# values (41–50), saturation with plagioclase and amphibole), basaltic and basaltic andesite Kizimen inclusions in their turn are fractionated compared with the primary mantle melts and to various degrees are contaminated with more acidic materials of hosting lavas. At the same time dacite and andesite lavas are contaminated with more mafic materials of inclusions. The processes of mixing basalt and dacite materials are indicated by the so-called banded lavas, in which bands vary from tens of centimeters to almost indistinguishable mixed patterns. Numerous basalt inclusions inside andesite basalt inclusions with boundaries that are often diffuse (Fig. 2a) indicate the repeated mixing of melts of different compositions. Consequently, both acid lavas and the mafic inclusions in them are hybrids that formed during the mixing of more extreme end members that are not found between the volcano rocks. Against the background of regional geochemical variations of Kamchatka's rocks from the front to rear arc with an alkalinity change of more than 4 times and changes in the concentrations of most noncoherent elements by 2–4 times [Ivanov, 2008; Ponomareva et al., 2008; Churikova et al., 2001] the lavas of Kizimen volcano occupy an intermediate position between volcanic rocks of EVF and CKD, not only in the major elements (Fig. 3a), but in all traces.

The Sr and Nd isotope ratios in the three most mafic rocks of the volcano are very similar (Fig. 3c) and vary insignificantly ($^{87}Sr/^{86}Sr$: 0.703352-0.703370, $^{143}Nd/^{144}Nd$: 0513045–0.513048). Figurative points of Kizimen volcano basalts occur within the field of EVF, CKD, and Sredinnyi Ridge (SR) of Kamchatka [Ponomareva et al., 2008; Churikova et al., 2001b] and are the most primitive in these parameters.

Therefore, the rocks of the Kizimen volcano have the following characteristic features: (1) dacite and andesite lava flows contain many inclusions of basalt and basaltic andesite composition; (2) banded mixed lavas are abundant; (3) rare-earth element distribution curves of dacite lavas and basalt inclusions in them intersect; and (4) the Sr–Nd isotope systematics of rocks and inclusions in these rocks do not suggest contamination with crustal material.

4. THE RESULTS OF THE GEOCHEMICAL ANALYSIS OF PLAGIOCLASES

Plagioclase phenocrysts were studied in detail in three samples: (a) the dacite lava of a near-summit flow (sample # KIZ-07, $SiO_2 = 60.1$); (b) basaltic andesite inclusion in this lava (sample # KIZ-07/1, $SiO_2 = 52.9$); and (c) basalt inclusion from another near-summit flow (sample # KIZ-01/1, $SiO_2 = 49.7$). Pl phenocrysts in both host rock and basalt inclusions are represented by two generations: the Pl-1 phenocrysts are unresorbed grains with clear-cut contours and well-expressed growth zones (Figs. 4a, 5a), and the Pl-2 phenocrysts are phenocrysts that resorbed to various degrees, in which resorption zones sometimes occupy more than 50% of a crystal (Figs. 4b, 5b). As seen in reflected light, the unresorbed crystals from mafic inclusions involve nearly no zoning (Fig. 4a), while unresorbed grains in lavas have fine zoning with zones of partial dissolution and healing (Fig. 5a). The inner parts of resorbed crystals in both dacites and in inclusions are multizonal and are similar to non-resorbed crystals of dacite lavas by their petrographic features.

Several crystals of each plagioclase variety from "acid host lava–mafic inclusion" pairs were analyzed for major (Al, Si, Na, Ca, and K) and trace (Ba, Sr, Mg, Fe, and Ti) elements at sites 2 to 5 microns in size along profiles from the center to the margin of phenocrysts. The results of the analyses were given in [Churikova et al., 2007] and are displayed for four representative grains in Figs. 4 and 5. Non-resorbed phenocrysts of plagioclase (Pl-1) from dacite lavas and from mafic inclusions in them fundamentally differ in composition, while the resorbed varieties (Pl-2) are surprisingly similar in chemical composition in all the rocks we studied.

4.1. The Generation of Pl-1 Crystals in Basalt Inclusions

Non-resorbed plagioclase crystals from basalt inclusions are characterized by very insignificant zoning in the center of a crystal (Fig. 4a) and the most mafic composition among all the studied varieties of plagioclases (An_{84}–An_{90}, see insert in Fig. 4a). The cores of some crystals contain traces of melting (dotted line, Fig. 4a) and of subsequent healing with hornblende (white fragments in the core center, Fig. 4a), seldom with magnetite and also with segments of more acid plagioclase (An_{77}) (Fig. 4a). The inner parts of non-resorbed plagioclase crystals from mafic inclusions typically have low Ba concentrations (0–50 ppm) and lower Sr con-

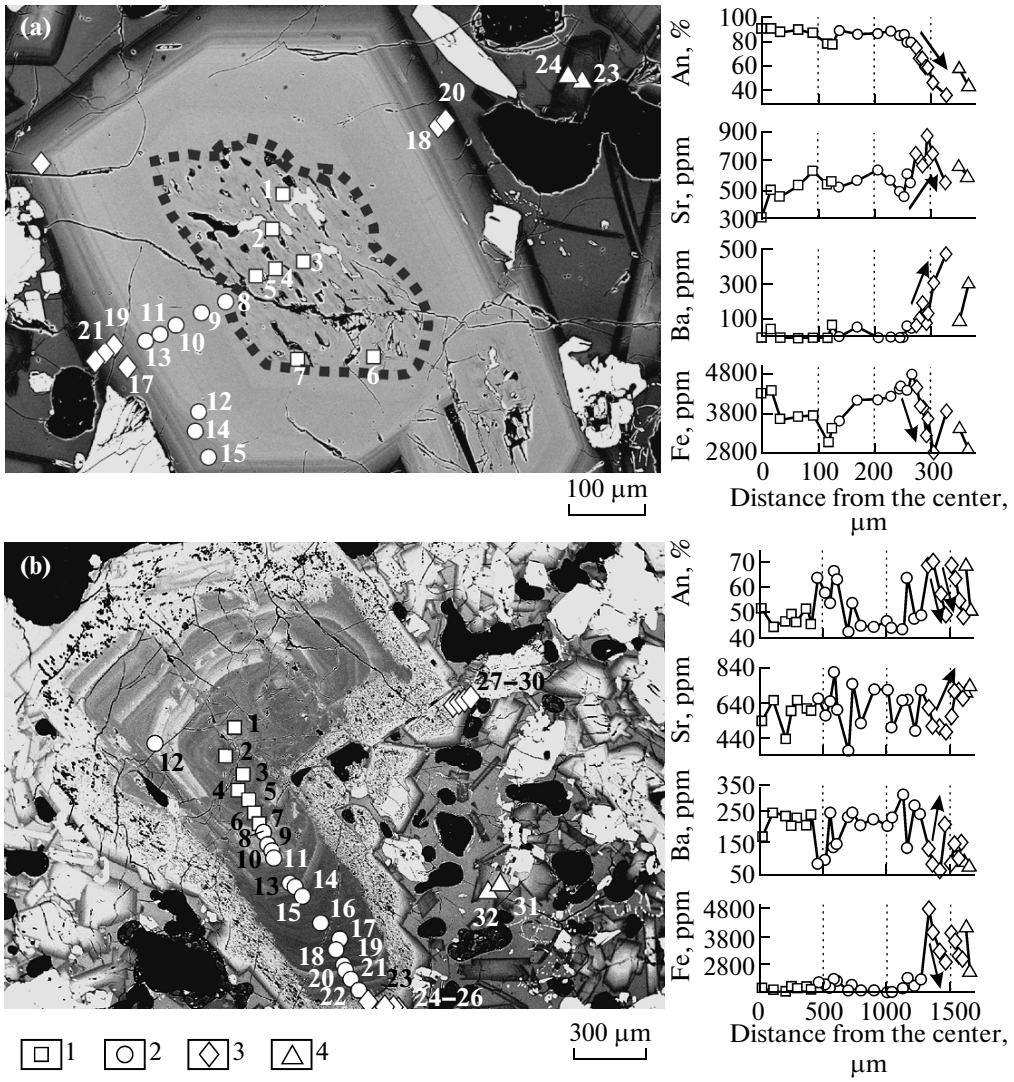

Fig. 4. Electron microprobe profile of quantative point determinations in typical plagioclases from basalt inclusions in Kizimen lavas. Numbers designate successively analyzed points from the core to rim of grains (a) in non-resorbed plagioclase (the grain center is marked by dotted line) and (b) in resorbed plagioclase. The inserts display the variation of the An, Sr, Ba, and Fe concentrations along the profile. Several grains of plagioclase microlites that were found near the studied phenocrysts were analyzed for comparison. Arrows indicate geochemical variations at the grain margins corresponding to the last stage of magma mixing before the eruption. (1) phenocryst centers, (2) intermediate zones of phenocrysts, (3) marginal zones of phenocrysts, (4) microlites. Point 23 in Fig. 4b corresponds to the resorption zone.

tents (mostly 300–550 ppm), as well as high concentrations of Fe (up to 5000 ppm) and Mg (300–500 ppm). The marginal zones of these crystals sharply differ from the inner and intermediate zones. In marginal zones (varying from a few microns to 100 microns) a sharp drop (to An_{36}) of the anorthite component is noted, Sr and Ba contents increase to 900 and 500 ppm, respectively, and the concentrations of Fe and Mg decrease to 2800 ppm and 200 ppm, respectively (Fig. 4a). The compositions of the outer zones of these crystals are similar in chemical composition to the nearest microlites.

4.2. Generation of Pl-1 Crystals in Dacite Lavas

Non-resorbed plagioclase crystals from dacite lavas typically have well-expressed zoning and are often rather large in size (up to 2 cm) (Figs. 2b, 5a). In contrast to Pl-1 phenocrysts in basalts, the central and intermediate zones of Pl-1 from dacite lavas have rather low calcium contents (An_{40}–An_{50}) and high Sr (500–750 ppm) and Ba (150–300 ppm), as well as low values of Fe (1500–2000 ppm) and Mg (100–150 ppm). Due to the fine zoning of these crystals, the element distribution curves are strongly jagged, reflecting the variations of chemical composition in different zones of the same crystal (Fig. 5a). Similarly to Pl-1 crystals from basalt

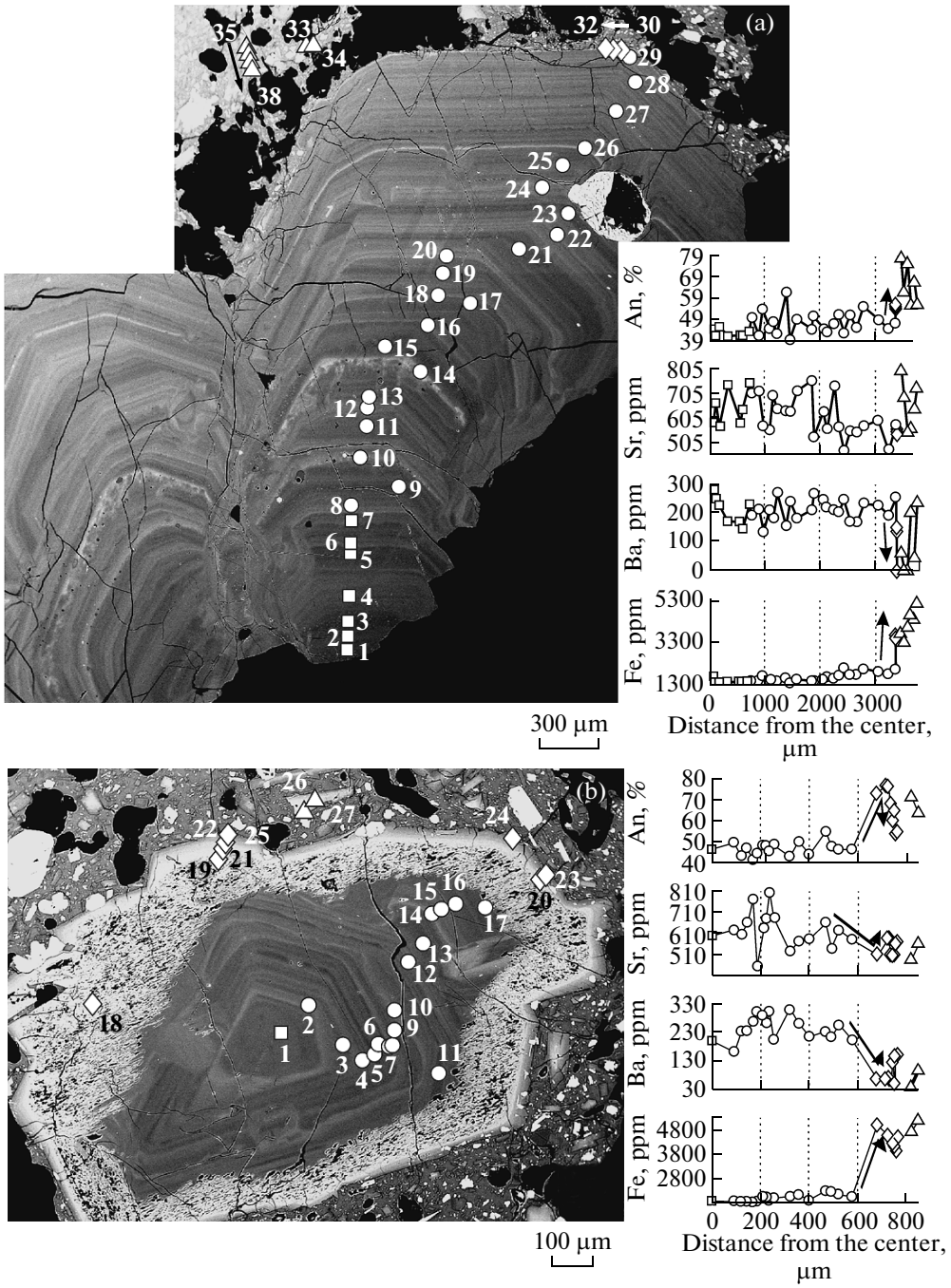

Fig. 5. An electron-microprobe profile of quantative point determinations in typical plagioclases from dacite lavas of Kizimen Volcano. The numbers designate successively analyzed points from the core to rim of grains (a) in non-resorbed plagioclase sized more than 2 cm and (b) in resorbed plagioclase (resorption rim is more than 0.1 cm). Changes in An, Sr, Ba and Fe concentrations from core to rim are shown in the inserts. Several grains of plagioclase microlites found near the studied phenocrysts were analyzed for comparison. Point 18 in Fig. 5b corresponds to the resorption zone. For legend see Fig. 4.

inclusions, the margins of Pl-1 crystals from dacite lavas notably differ from the inner and intermediate zones, although the trend of the change is directly opposite: an increase in the anorthite component in marginal zones (up to An_{55}), enrichment in Fe (up to 3500 ppm) and Mg (up to 300 ppm) and depletion in Ba (<100 ppm) and Sr (up to 500 ppm) (Fig. 5a). The nearest microlites are similar in composition to phenocryst rims.

4.3. The Generation of Pl-2 Crystals in Inclusions in Dacite Lavas

As mentioned above, resorbed plagioclase crystals (Pl-2) from dacite lavas and basalt inclusions are surprisingly similar to each other, both in morphology and chemical composition. Three major zones are clearly defined in the structure of these crystals: (I) an inner

one, with well-expressed zoning, (II) a resorption zone that varies from 50 to 200 microns, and (III) an outer rim up to 50 microns (Figs. 4b, 5b). The inner zones of Pl-2 plagioclases are analogous in chemistry to the inner zones of Pl-1 plagioclases from dacite lavas, i.e., they are characterized by low values of An, Fe, and Mg with relatively high concentrations of Ba and Sr. The plagioclase in the resorption zone is more mafic, with a sharply increased content of the An component (up to An_{80}) and concentrations of Fe and Mg (up to 5000 ppm and 550 ppm respectively) and decreased contents of Sr and Ba. The plagioclase in the marginal zone III again becomes more acidic, but the content of An remains higher than in the central parts of grains. Microlites situated close to resorbed grains vary in chemical composition and correspond to the chemistry of Pl-2 plagioclase in zones II and III.

5. RESULTS AND DISCUSSION

The diagram that shows the Mg concentration in relation to the anorthite component in plagioclase (Fig. 6) clearly demonstrates two fields that form two zones marked as the cores of mafic and acid plagioclases. The cores of non-resorbed grains from basalt inclusions are the most mafic (An_{75}–An_{94}) and the richest in Mg (300–550 ppm) compared with all the other crystals (Figs. 4, 5, 6). These high-anorthite plagioclases with high concentrations of magnesium were probably growing in the most mafic high-magnesia melt of basalt composition. They are never resorbed and very rarely occur in host rocks. In contrast to them, the central and intermediate zones of non-resorbed crystals from host rocks are analogous to central and intermediate parts of resorbed crystals, both from dacite host rocks and basalt inclusions (Figs. 4b, 5, and 6) and consist of low-anorthite plagioclases (An_{40}–An_{50}) with similar concentrations of microcomponents (including low Mg content), indicating their generation from a single low-magnesium dacite melt. These low-anorthite plagioclases probably grew from an evolving acid melt and occur both in hosting dacite lavas and in basalt inclusions.

The compositions of the intermediate zones and margins of crystals provide evidence of the different histories of the melts from which they crystallized. Non-resorbed plagioclases from inclusions demonstrate a typical trend of crystallization differentiation (Fig. 6b, trend I) with a decrease of An and Mg contents from the center to the margin of a crystal. The intermediate and marginal zones of non-resorbed plagioclases from host rocks form two trends. One of them coincides with trend I, while the other (Fig. 6b, trend II) consists in an increase of the An component from the center to the margin with constant Mg concentration. These two fundamentally different trends suggest different governing processes.

Trend I may be not only the classical trend of mafic melt differentiation, but also a trend of mixing acid and mafic melts with subsequent growth of the intermediate and marginal parts of crystals from the mixed melt. Mixing processes are also indicated by the fact that all acid plagioclases (including Pl-1 from hosting dacite and Pl-2 from both dacite lavas and basalt inclusions) demonstrate increasing An content from the core to the margin (Fig. 6b). Fractional crystallization without mixing would have resulted in an increase in only the plagioclase acidity.

The abundance of resorbed plagioclase phenocrysts in both rocks also indicates the mixing of a mafic and an acid melt. During mixing of low-temperature dacite lavas that contain plagioclase phenocrysts with a high-temperature basalt melt these crystals occur in an overheated environment. This causes dissolution of the margins of previous plagioclase crystals and their replacement with matrix structures of more mafic plagioclase with the formation of the resorption zone. In this zone, the plagioclase composition is characterized by the highest (for this crystal) values of An and Mg with the lowest concentrations of Ba and Sr (Fig. 5b). The resorbed plagioclases then overgrew a rim that was in equilibrium with the new hybrid melt that was intermediate in composition between basalt and dacite. Plagioclase microlites grew from the same melt; this is why they are similar to the rims of phenocrysts.

The intermediate zones of all (resorbed and non-resorbed) low-An plagioclases reveal a well-expressed zoning: light segments of plagioclase growth have higher An contents, while dark ones show lower concentrations (Fig. 5a). This zonality is clearly detected by increasing Mg and Fe and decreasing Ba and Sr in light plagioclase zones and forms the respective saw-toothed distribution of trace elements. Consequently, the process of mixing acid and mafic melts took place repeatedly in the course of the system's evolution. Addition of the last portion of basalt melt possibly triggered the eruption, which is recorded in the sharp change of the composition in the marginal zone of plagioclase crystals.

As for plagioclase crystals that formed from a high-temperature basaltic melt (Pl-1 in basalt inclusion, see Fig. 4a), they didn't dissolve during mixing with low-temperature dacite magma. However, mixing with an acid melt is indicated by development of acid marginal zones around high-An inner parts of the crystals, namely, zones with decreased contents of An, Mg, and Fe and increased Ba and Sr (Fig. 4a). The Pl-1 crystals from basalt inclusions are little affected by the addition of acid material, which explains their poor zonality and rather flat profiles of microelement distribution.

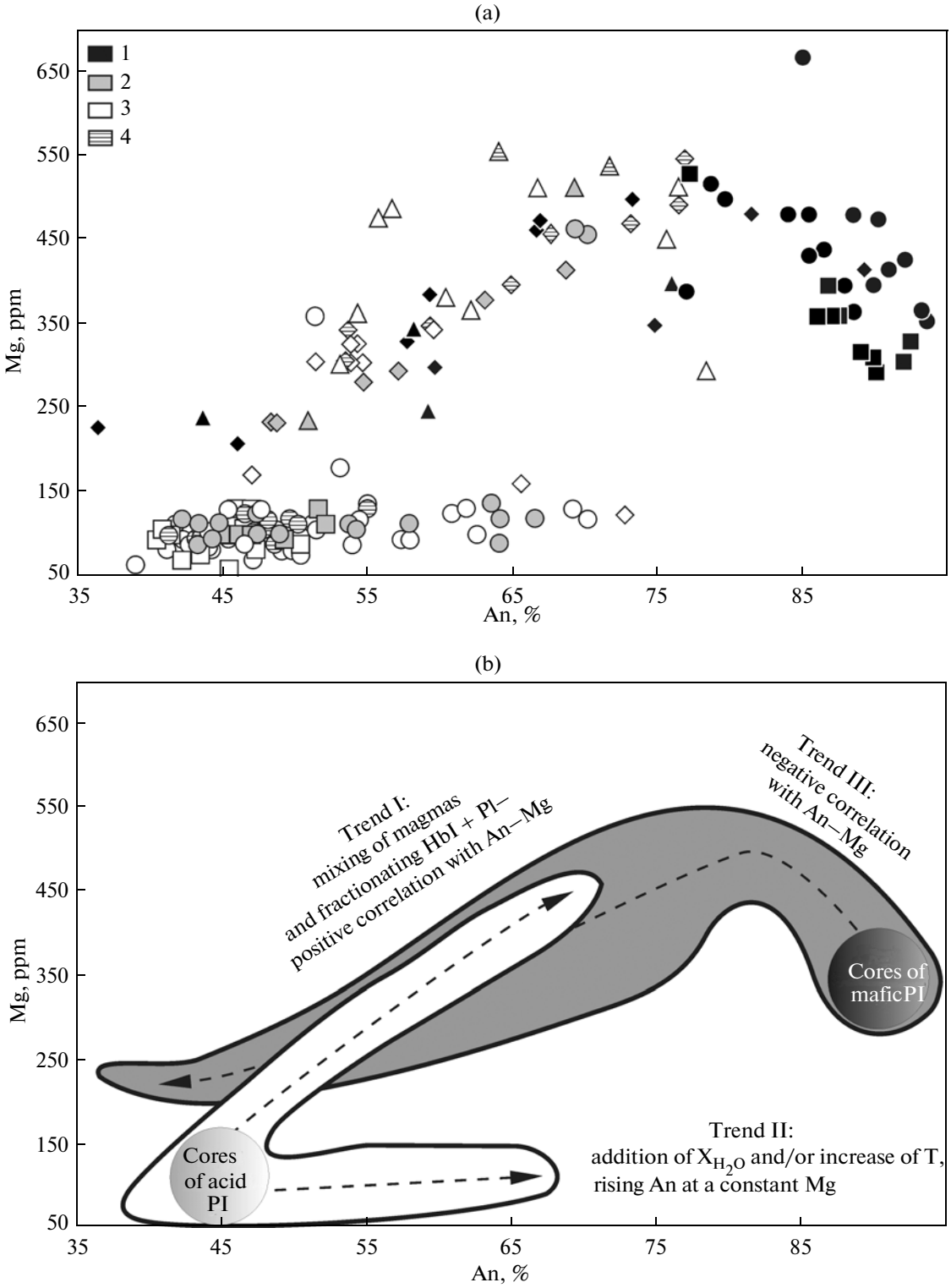

Fig. 6. A diagram of the Mg content in plagioclase versus its An number (a). The symbol shape designates the positions of points inside a crystal: squares denote the center, circles denote intermediate zones, diamonds denote rims, and triangles denote microlites. (1) Pl-1 from mafic inclusions; (2) Pl-2 from mafic inclusions; (3) Pl-1 from host dacite lava; (4) Pl-2 from host dacite lava. The scheme of crystal evolution is shown by arrows from the centers to the margins of the grains (b). The gray fields correspond to high-An (mafic) plagioclases from basalt and basaltic andesite inclusions in lavas; the white fields show the evolution of low-An (acid) plagioclases from both lavas and their inclusions.

As well, the abundance of banded lavas and inclusions of basaltic andesites and basalts in dacite (Fig. 2) is also a reliable sign of melt mixing; the presence of several generations of inclusions (the occurrence of more mafic inclusions in less mafic ones) attests to the multistage character of these process (Fig. 2b).

In Fig. 6 the cores of low-An plagioclases occur on the extension of trend I, which suggests that mixing melts might be lavas of a single source with different degrees of differentiation. This is supported by the similar isotope characteristics of the dacites and basalts (Fig. 3c), as well as by the similarity of the geochemical characteristics in the trace element composition. This similarity is observed on spider diagrams, in which all the minima and maxima of both rock types coincide.

Trend II in Fig. 6b demonstrates many repeated changes in the An content in plagioclase without corresponding changes in Mg concentration. This behavior of plagioclase is explained by an increase of temperature in the magma chamber with no changes in the chemical composition of the melt. An increase in temperature is indicated by crystallization of the more mafic plagioclase; the stability of the chemical composition of the system is suggested by the constant concentration of Mg in the plagioclase, which is largely controlled by the Mg concentration in the melt. The temperature increase may result from the heating of a dacite melt by the intrusion of a high-temperature basalt magma. This may not happen in the boundary zone where the two melts mix but at some distance from it where no physical or chemical mixing occurs but the temperature increases. A similar effect must be observed as well in the case of greater water presence in the melt [Volynets et al., 1977].

Finally, trend III in Fig. 6 is characterized by an increase of Mg and to a lesser extent, by an increased Fe content [Churikova et al., 2003, 2007] with a decreasing An-component in plagioclases. We observed such Mg behavior only in the central and intermediate parts of high-anorthite non-resorbed plagioclase grains from basalt inclusions (Fig. 6b). It is logical to assume that these, the most mafic plagioclases, must have originated from the most primitive melts. In order to explain the negative correlation of magnesium and anorthite in crystals that correspond to trend III the following three scenarios are considered.

5.1. Long-Term Replenishment of the Magma Chamber by Hot High-Mg Melts with the Accumulation of Magnesium

The existence of resorption structures in some cores of Pl-1 crystals from basalt inclusions (Fig. 4a) may suggest such mixing with a hotter melt events at the earlier stages of plagioclase crystallization. Nevertheless, the negative correlation between An, Mg, and Fe in Pl-1 plagioclases is noted not in the cores only, but also in the intermediate zones of phenocrysts with no resorption. Therefore this scenario should be excluded from consideration.

5.2. Crystallization of Plagioclase as the First and Single Phase

If the coefficient of magnesium distribution Kd_{Mg} in the plagioclase–melt system is not changing significantly [Bindeman et al., 1998] it is logical to assume that during the growth of crystals with a negative An–Mg correlation the melt would be enriched in magnesium. The major rock-forming minerals in the volcano rocks are olivine, pyroxene, hornblende, and plagioclase. The last mineral occurs in all the rock varieties. The contents of olivine and pyroxene decrease while hornblende increases from basalts to dacites; however, hornblende grains are also found in mafic rocks. The same minerals occur as microlites in the groundmass, which is crystallized to a different degree. Because during crystallization of Ol, Cpx, and HbI the magnesium concentration in a melt will drop dramatically, enrichment of a melt with this element is possible in the process of fractional crystallization of only plagioclase as the first and single phase. This explanation may be tested by simulation calculations if the temperature and pressure of the crystallization are known.

In order to identify the conditions of crystallization inside a magma chamber and the composition of a hybrid magma just before an eruption a series of petrographic experiments was performed in the Geophysical Institute of the University of Alaska, (Fairbanks, United States) [Browne et al., 2006, 2010]. Natural samples of dacites from Kizimen volcano reveal a stable mineralogical association: Pl + Opx + Hbl + Mt + Ilm. According to the magnetite–ilmenite geo thermometer [Stromer, 1983], the equilibrium temperature of crystallization was calculated as 815–825°C. The entire mineralogical association of Kizimen dacite was obtained exactly at this temperature in the experiments (Fig. 7a). All the experiments were carried out at the temperatures and pressures at which plagioclase was stable. Results of analyses of compositions of experimentally obtained plagioclases in comparison with the natural plagioclase rims of studied dacites are shown in Fig. 7b. It is clearly seen that for an equilibrium temperature of crystallization of 815–820°C, the natural compositions occur between the experimental compositions observed in the experiments at 125 MPa and 150 MPa, supposing equilibrium pressure about 125 MPa and temperature close to 820°C. Under the same conditions the glass compositions that were obtained in the experiments correspond to compositions of natural residual melts (see Fig. 7c; data for SiO_2 and FeO are shown).

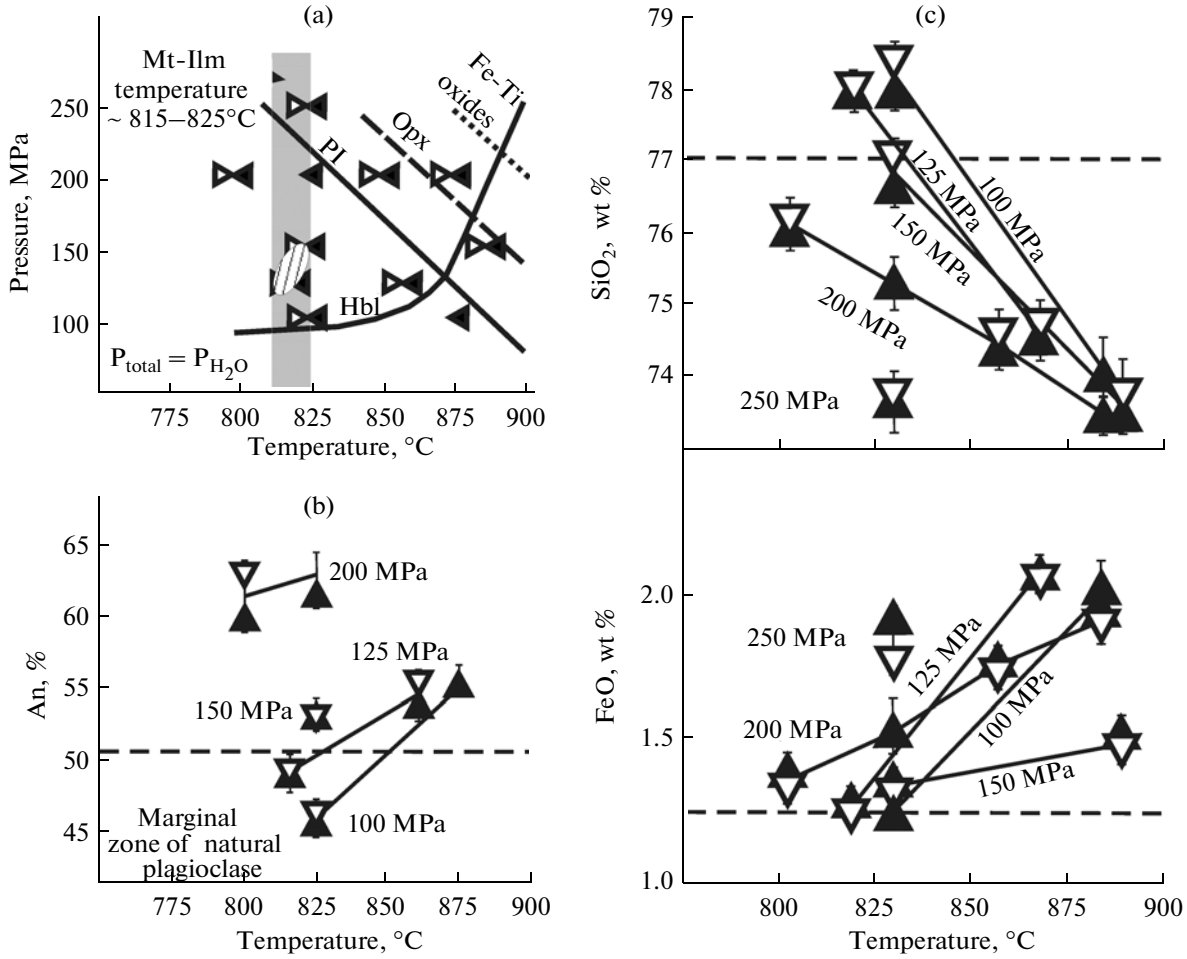

Fig. 7. The results of petrographic experiments for rocks of Kizimen Volcano (based on the data of [Browne et al., 2006, 2010]). A phase diagram (7a) that shows the stability fields for the mineral associations of Kizimen dacites and the P–T conditions of the experiment. The open and filled triangles denote experiments on crystallization and melting, respectively. The solid and dotted lines are lines of the entry of corresponding rock-forming minerals. The hatched field designates the P–T stability conditions for Kizimen dacite immediately before eruption obtained on the basis of experimental data, geothermometry, phase stability, and the compositions of coexisting glass and minerals. The compositions of plagioclases (7b) in comparison with the marginal part of the natural plagioclase from Kizimen dacite (dotted line) for different P–T conditions. Comparison of glass compositions (c) that were obtained at different temperatures and pressures with natural glass of Kizimen dacite (dotted line). The solid lines show experiments that were performed at a constant pressure.

Therefore, experiments showed that the last equilibrium of dacite lava of Kizimen volcano happened at a pressure of about 125 MPa and temperature of about ~820°C (Fig. 7). With these parameters under experimental conditions, the complete mineral association of the studied dacite (Fig. 7a), the composition of the natural plagioclase (Fig. 7b), and the composition of the residual melt (Fig. 7c) were reproduced.

Based on the obtained experimental data and supposing that the magma chamber remained at the same depth in the course of melt evolution we calculated the model of fractional crystallization for the most mafic melt of the basalt inclusion of Kizimen volcano (see Table 1, high-Al basalt KIZ-01/1) using the COMAGMAT program package [Ariskin et al., 1993] under the following conditions: P = 125 MPa, H_2O = 1%, buffer NNO [Churikova et al., 2007].

As seen from Fig. 8, the model compositions that were obtained in calculations are close to the observed compositions of Kizimen volcano magmas. Although the numerical model reproduces the increase in Mg and Fe in the melt with a simultaneous decrease of An in plagioclase at the earliest stages of crystallization (Fig. 6a, 6b, 6f), the trends of the volcanic rocks do not exhibit corresponding maxima in the MgO and FeO – SiO_2 diagrams. The observed compositions of olivine and pyroxene are reproduced well in the model (model compositions – $Fo_{78.5\text{-}76}$ and $En_{43\text{-}46}Fs_{12\text{-}17}Wo_{40\text{-}42}$, natural compositions [Ivanov, 2008; Melekestsev et al., 1992] $Fo_{79\text{-}75}$ and $En_{44}Fs_{16}Wo_{40}$), but the most calcic

The chemical and isotope compositions of Kizimen volcano rocks

	TAM-01	KIZ-01	KIZ-01/1	KIZ-02	KIZ-04	KIZ-05	KIZ-07	KIZ-07/1	KIZ-08	KIZ-09
SiO_2	51.40	63.60	49.70	62.40	60.60	56.20	60.10	52.90	57.70	63.30
TiO_2	0.83	0.58	1.22	0.65	0.66	0.89	0.77	1.10	0.93	0.61
Al_2O_3	15.76	16.17	18.84	16.54	17.29	17.26	16.87	18.35	17.12	16.10
Fe_2O_3	9.37	2.41	5.32	2.69	2.75	3.43	3.83	4.22	3.63	2.41
FeO	0.43	3.03	5.56	3.21	2.53	4.75	3.09	5.30	4.19	3.10
MnO	0.19	0.13	0.19	0.14	0.13	0.17	0.15	0.19	0.17	0.13
MgO	8.43	2.44	5.20	2.67	2.65	3.99	3.10	4.41	3.58	2.41
CaO	9.23	5.34	9.25	5.89	5.63	7.17	6.34	8.48	7.07	5.42
Na_2O	2.72	3.69	2.74	3.73	3.61	3.27	3.58	3.26	3.44	3.74
K_2O	0.73	1.66	0.76	1.57	1.48	1.14	1.46	0.89	1.25	1.72
P_2O_5	0.23	0.16	0.17	0.15	0.19	0.16	0.16	0.19	0.18	0.15
LOI	0.66	0.61	0.73	0.40	2.19	1.17	0.38	0.50	0.57	0.42
Total	99.98	99.82	99.67	100.04	99.70	99.60	99.83	99.79	99.82	99.52
Li	7.9	16.3	14.2			10.2				
Be	0.51	0.79	0.52			0.63				
Sc	31	15	26	17	15	21	18	26	24	15
V	221	114	300	137	146	208	163	250	199	115
Cr	481	17	15	16	26	10	12	11	19	13
Co	36	14	30	18	14	29	17	26	21	13
Ni	166	0	2	0	1	7	0	0	0	0
Zn	79	55	79	61	57	68	63	74	65	55
Ga	15	16	17	16	15	17	15	18	16	15
Rb	15	38	14	34*	32*	26	31*	17*	25*	41*
Sr	380	319	370	328	318	330	320	368	325	304
Y	16	16	21	19*	15*	20	22*	24*	22*	18*
Zr	86	121	86	124	115	102	117	96	117	126
Nb	2.4	4.2	2.9	5.0*	6.0*	3.5	4.0*	3.0*	4.0*	4.0*
Cs	0.50	1.5	0.52			0.47				
Ba	358	676	310	593	608	458	567	376	451	655
La	7.62	10.16	5.85			7.73				
Ce	19.02	22.39	15.18			19.37				
Pr	2.69	3.32	2.34			2.76				
Nd	13.10	13.54	11.99			12.79				
Sm	3.72	2.89	3.36			3.23				
Eu	1.11	0.95	1.14			1.04				
Gd	3.29	2.58	3.28			2.97				
Tb	0.52	0.36	0.54			0.44				
Dy	3.38	2.28	3.33			2.94				
Ho	0.67	0.55	0.74			0.65				
Er	2.06	1.46	2.18			1.85				
Tm	0.32	0.20	0.30			0.26				
Yb	2.05	1.39	2.00			1.72				
Lu	0.31	0.24	0.29			0.28				
Hf	2.27	1.91	1.99			1.88				
Ta	0.19	0.21	0.17			0.17				
Tl	0.03	0.27	0.10			0.10				
Pb	2.15	5.30	1.95			3.01				
Th	0.91	3.19	1.02			1.42				
U	0.45	1.45	0.49			0.79				
$^{87}Sr/^{86}Sr$			0.703352							
$^{143}Nd/^{144}Nd$			0.513045							
$^{206}Pb/^{204}Pb$										
$^{208}Pb/^{204}Pb$										
$^{207}Pb/^{204}Pb$										

Table 1. (Contd.)

	KIZ-11	KIZ-17/2	KIZ-18	KIZ-19	KIZ-21	KIZ-22	KIZ-23	KIZ-24	KIZ-24/1
SiO_2	55.70	57.30	61.60	50.30	55.40	61.30	63.60	54.70	51.60
TiO_2	0.97	0.84	0.67	1.20	1.07	0.64	0.58	1.03	1.28
Al_2O_3	17.61	17.19	16.50	16.50	17.22	16.54	16.14	17.44	17.91
Fe_2O_3	2.90	2.76	2.46	2.97	3.14	3.08	2.60	3.07	4.29
FeO	5.52	4.84	3.52	8.01	4.96	2.91	2.74	5.49	5.78
MnO	0.17	0.17	0.14	0.21	0.18	0.13	0.13	0.17	0.19
MgO	4.16	4.14	2.72	5.22	3.05	2.86	2.37	4.16	4.42
CaO	7.70	7.24	5.84	9.59	7.36	5.71	5.32	8.18	9.13
Na_2O	3.30	3.33	3.76	2.70	3.66	3.51	3.69	3.18	3.03
K_2O	1.14	1.28	1.52	0.71	1.37	1.40	1.66	1.10	0.87
P_2O_5	0.17	0.18	0.15	0.21	0.26	0.16	0.15	0.17	0.19
LOI	0.33	0.34	0.71	1.87	1.78	1.15	0.61	0.47	0.85
Total	99.67	99.60	99.59	99.48	99.46	99.39	99.60	99.16	99.53
Li				3.8				8.5	11.7
Be				0.44				0.56	0.56
Sc	21	22	18	35	26	16	13	22	33
V	220	190	133	316	187	130	108	246	324
Cr	16	47	20	42	11	34	19	24	21
Co	27	20	21	37	20	14	13	27	27
Ni	6	20	1	25	0	8	2	2	0
Zn	71	76	58	94	83	60	57	72	80
Ga	16	17	16	18	19	15	15	19	17
Rb	24*	28*	33*	9	15*	30*	36*	21	16
Sr	332	359	324	276	299	341	320	328	335
Y	23*	24*	20*	32	34*	15*	19*	20	23
Zr	98	124	124	104	140	109	124	99	90
Nb	4.0*	4.0*	3.0*	4.1	6.0*	3.0*	4.0*	3.1	3.2
Cs				0.31				0.79	0.59
Ba	459	466	606	164	200	591	669	419	323
La				6.49				6.52	7.02
Ce				19.11				16.57	18.10
Pr				2.73				2.83	2.59
Nd				13.11				12.73	13.08
Sm				3.86				3.25	3.91
Eu				1.14				1.08	1.27
Gd				4.04				3.12	3.53
Tb				0.70				0.47	0.63
Dy				4.37				3.08	3.88
Ho				0.94				0.76	0.75
Er				2.89				1.97	2.23
Tm				0.42				0.27	0.34
Yb				2.77				1.72	2.38
Lu				0.42				0.30	0.32
Hf				2.80				2.10	2.17
Ta				0.21				0.14	0.19
Tl				0.05				0.09	0.10
Pb				2.03				2.73	2.63
Th				0.59				1.57	0.91
U				0.38				0.77	0.61
$^{87}Sr/^{86}Sr$								0.703347	0.70337
$^{143}Nd/^{144}Nd$								0.513048	0.513047
$^{206}Pb/^{204}Pb$									18.32
$^{208}Pb/^{204}Pb$									38.033
$^{207}Pb/^{204}Pb$									15.5

Note: Major elements, Sc, V, Cr, Co, Ni, Zn, Ga, Sr, Zr, and Ba as well as the elements marked by asterisks were determined by the XRF method; the other concentrations were obtained by the ICP-MS method. Samples KIZ-17/2, KIZ-19, KIZ-21, and KIZ-22 were taken from the ancient basement of the volcano and are not considered in this study. The rest of the samples are of Q_4 age.

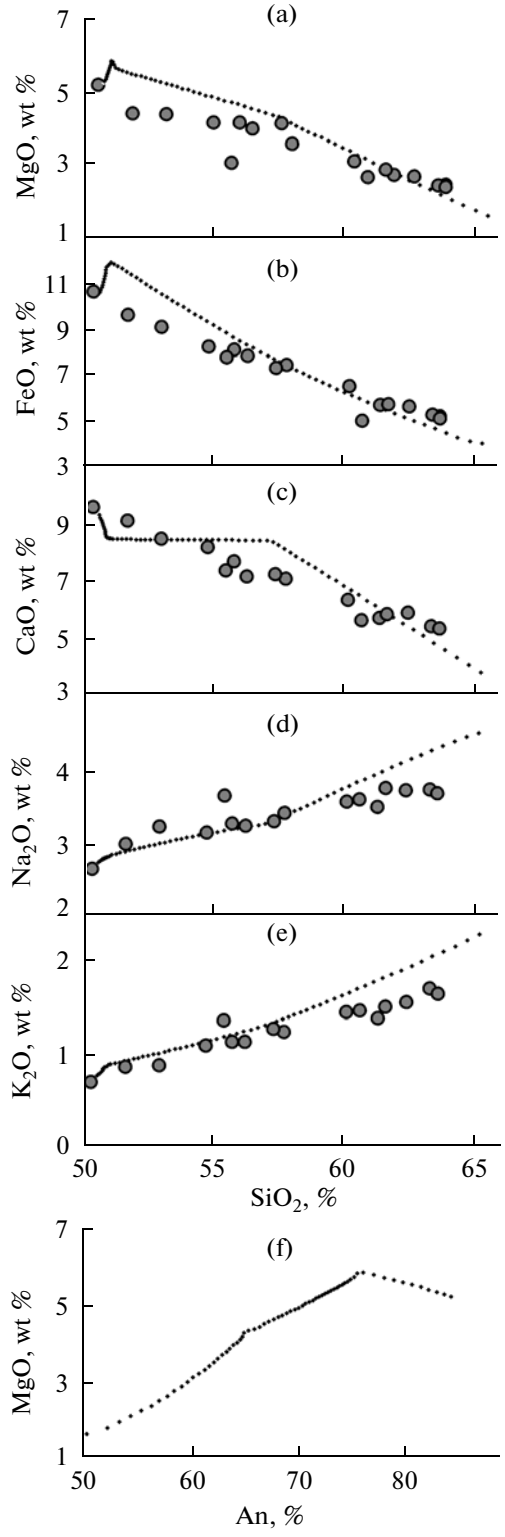

Fig. 8. A numerical model (dotted line) of the fractional crystallization of Kizimen basalt magma (sample KIZ-96-01/1) compared with the actual rock compositions (gray circles). The calculations were carried using the COMAGMAT program [Ariskin et al., 1993] with the following parameters: P = 125 MPa, NNO buffer and H_2O = 1%. Due to the fractionation of Pl at the first stages of crystallization, the residual melt is enriched in MgO.

plagioclase in the calculations is An_{84-85}, while cores and intermediate Pl-1 zones from basalt inclusions exhibit values up to $An_{93.6}$ (see Table 2 in [Churikova et al., 2007]). Therefore, we believe that the composition that the calculation began with was not the primary one. Low values of MgO (4–5%), Ni (less than 2 ppm), Cr (11–20 ppm), and relatively high values of K_2O (0.9%) attest to the fact that the basalt inclusions themselves are already fractionated melts and the occurrence of resorption zones in Pl-1 cores and numerous inclusions inside the larger ones (Fig. 2b) provide evidence of repeated mixing processes in mafic magmas. Conditions in which Pl may crystallize as the first phase are very limited; according to our calculations this may take place only at pressures of 1–3 kbars (up to 10 km). In the case of crystallization from a parent melt with a higher magnesia concentration, such a scenario would be completely impossible.

Therefore, although the possibility of crystallization of plagioclase as the first phase from high-Al hybrid melts exists in principle, this process cannot control the distribution of MgO and FeO in the most sodic and the most calcic plagioclases.

5.3. The Nonlinear Behavior of the Kd_{Mg} Distribution Coefficient in the Melt–Plagioclase System

Sato [1989] noted that because of the kinetic disequilibrium distribution the coefficients measured in experiments may significantly differ from the equilibrium values recorded in real natural systems. The experimentally determined distribution coefficients Kd_{Mg} vary in narrow limits and are almost independent of the melt composition [Bindeman et al., 1998] based on the supposition of a positive correlation between An and Mg in plagioclases. Exactly this correlation is observed for relatively acid (Fig. 6b, trend I), but not for high-An plagioclases of Kizimen Volcano. It should be mentioned that most experimental works on the determination Kd_{Mg} and Kd_{Fe} have been carried out for plagioclases up to An_{85} [Severs et al., 2009], whereas trend III occurs in the area of An_{75-93}, where a negative correlation between An and Mg is clearly observed (Fig. 6b, trend III). This may indicate a nonlinear behavior of the Kd_{Mg} and Kd_{Fe} distribution coefficients in high-An plagioclases. Below, we will demonstrate that the negative correlation between An and Mg (Fe) is found not only on Kizimen volcano, but also in other even more primitive magmatic systems.

Melt inclusions were studied in the minerals of mid-ocean ridge basalts (MORB) from the Costa Rican Rift (hole 896A), where olivine, clinopyroxene and spinel were the first crystallizing phases [McNeill and Danyushevsky, 1996]. According to this data, the contents of An in plagioclases and concentrations of MgO and FeO

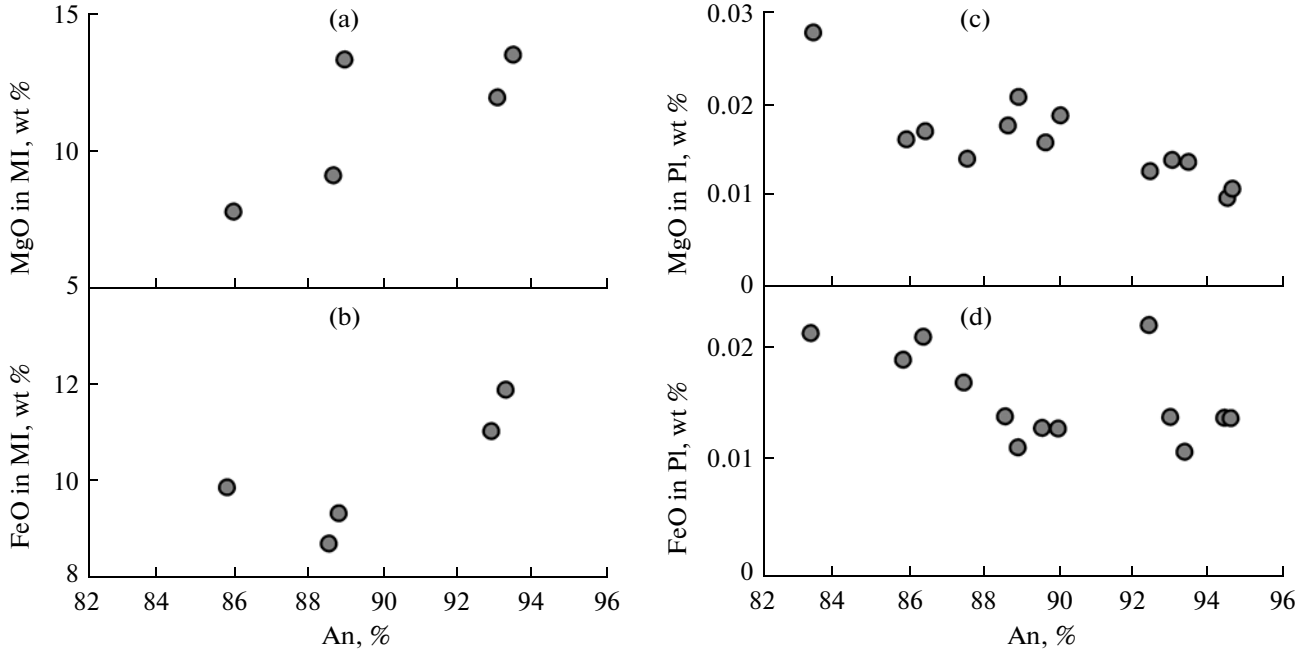

Fig. 9. Contents of MgO and FeO in melt inclusions in plagioclases (a, b) and in plagioclases (c, d) in relation to the An component of plagioclase from MORB basalts of the Costa Rican Rift (hole 896A; data from Tables 3 and 7 after [McNeill and Danyushevsky, 1996]). MI, melt inclusion.

in equilibrium melts display a positive correlation (see Tables 3 and 7 in [McNeill and Danyushevsky, 1996]). However, if we draw a diagram using the data from this paper, the trend of a negative correlation in all calcic (An_{83}–An_{95}) plagioclases (Fig. 9) will be clearly observed. Consequently, while the Mg content in the melt decreased, the concentration of Mg in the plagioclase that crystallized from this melt increased.

A similar behavior of FeO concentration, which showed a negative correlation with anorthite in plagioclases, has been noted in different volcanic rocks from Kamchatka and the Kuril Islands (see Fig. 3 from [Volynets et al., 1977]).

Therefore, we suppose that the negative correlation between the concentrations of Mg or Fe and the content of An in high-An plagioclases results from the nonlinear behavior of the Kd_{Mg} and Kd_{Fe} distribution coefficients in the plagioclase–melt system. This phenomenon was not noted before and requires experimental work to study the distribution coefficients in high-An plagioclases.

A schematic model of the magmatic system beneath Kizimen Volcano that illustrates these processes is displayed in Fig. 10. A mafic magma with high-An Pl-1 crystal intrudes into the dacite magma chamber with low-An Pl-1 crystals and the two magmas interact. This process generates hybrid magmas with two contrast zones, basalt and dacite, which exhibit the features of both chemical and thermal interactions (Fig. 2c). A Pl-1 crystal from dacite that penetrated into the mafic magma underwent thermal influence, which resulted in its dissolution and transition from Pl-1 generation into Pl-2. The new and more mafic hybrid melt formed around this plagioclase with the development of a calcic margin (Fig. 6, trend I). Some of such plagioclases return into the dacite magma, others remain in basalt inclusions.

At the contact with low-temperature dacite magma the Pl-1 crystals from high-temperature basalt do not change and are not resorbed. However, they are overgrown by the more acidic margin from the hybrid, more acidic, melt. These plagioclases are found in both basalt inclusions and in dacite lavas.

However, mixing processes were not effective enough to involve the entire volume of the magma chamber and result in its complete homogenization. Some portions of dacite magma had no direct contact with basalt melts and were not involved in chemical mixing processes; yet they experienced a thermal influence from the high-temperature melt. With increasing temperature the marginal zones of the acidic Pl-1 phenocrysts became high-An and formed trend II (Fig. 6).

We believe that the ascent and recharge of basalt magma into the dacite magma chamber of Kizimen volcano occurred rather often and resulted in the formation of a great number of basalt inclusions. The complex interaction between magmas at Kizimen shows much in common with analogous processes at Unzen volcano (Japan) [Eichelberger et al., 2000] and many other volcanoes (Fig. 10).

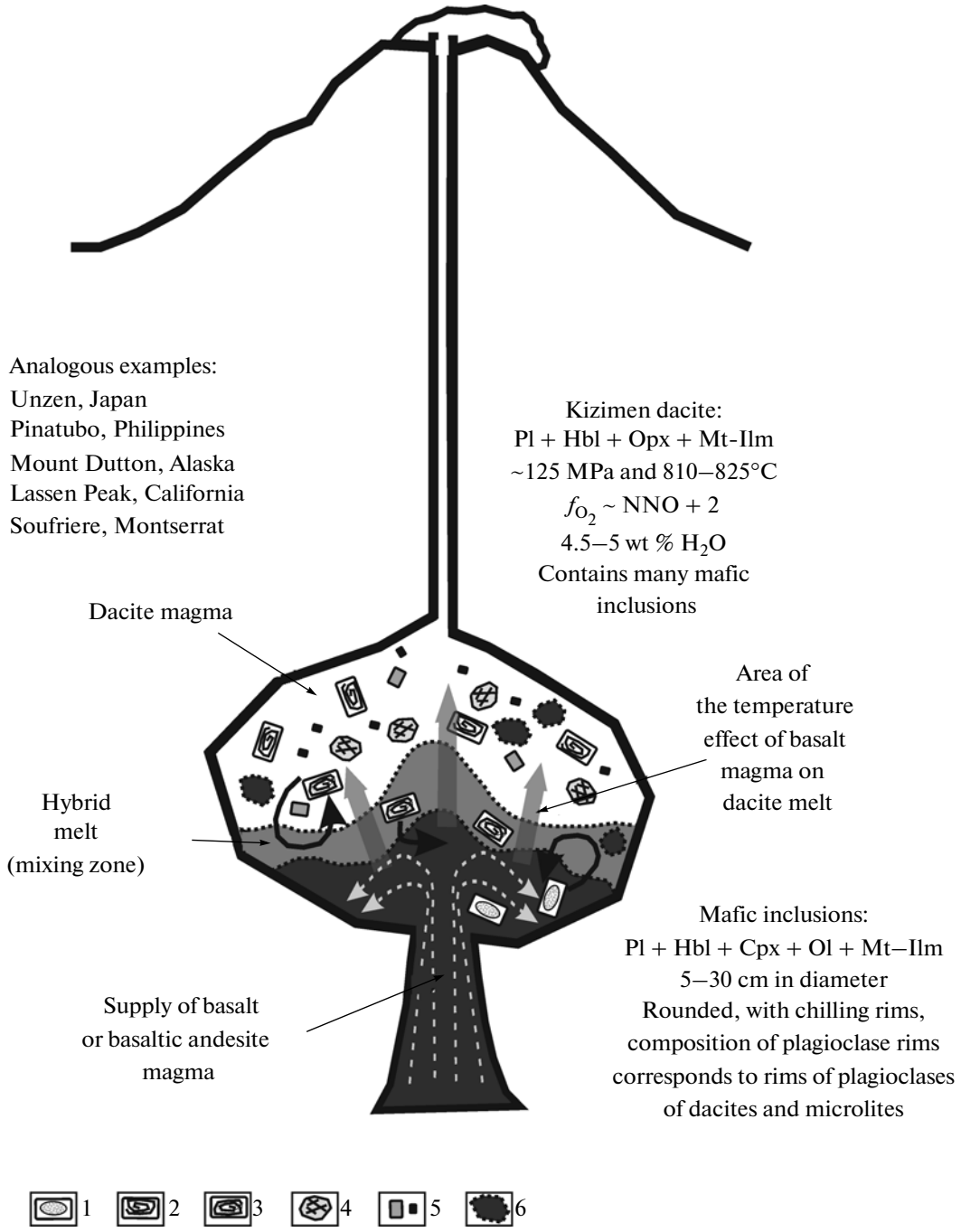

Fig. 10. A diagram of the processes in the magma chamber beneath Kizimen volcano. (1) non-resorbed plagioclase grains (Pl-1) in mafic magma; (2) non-resorbed plagioclase grains (Pl-1) in dacite magma; (3) resorbed plagioclase grains (Pl-2); (4) hornblende crystals; (5) subphenocrysts and microlites; (6) basalt melt inclusions in dacite. The black bent arrows indicate the main directions of plagioclase phenocryst movements inside the magma chamber.

CONCLUSIONS

This study of zoning in plagioclase phenocrysts from Kizimen volcano, as well as the distribution of major and trace elements in these crystals, suggest the following conclusions.

1. All the rocks of Kizimen volcano, including basalt and basaltic andesite inclusions in them, are hybrid and originated from mixing of mafic and acid melts in different proportions. These end members are probably derivates of one or several primary melts of similar composition and were formed in the course of fractional crystallization under extensive fractionation of amphibole.

2. The unusual negative correlation of MgO and An in high-An plagioclases may be explained by the non-

linear behavior of the Kd_{Mg} distribution coefficient in the plagioclase–melt system.

3. Recharge of basalt magma into the near-surface dacite magma chamber of Kizimen volcano occurred occasionally. The interaction of two magmas that were different in their compositions and physical properties was a complex process: while the chemical mixing of melts and crystals and subsequent crystallization of a hybrid melt occur widely in volcanic rocks, one may also note indications of heat transfer only (or addition of water), which is expressed in changes in the An component in plagioclase with a constant concentration of minor elements.

4. The trend within mafic enclaves toward more mafic compositions with time suggests that at present the reservoirs of acid and mafic melts are located in different parts of the system; the intrusion of basalt magma into the dacite reservoir is believed to be the trigger of the eruptions.

ACKNOWLEDGMENTS

We thank A.D. Babanskiy, D. Gardner, B.N. Gordeychik, A.N. Khrenov, and E.V. Sharkov for constructive suggestions that improved the manuscript.

This work was supported by Project Wo362/15-1+2, by the cooperative program of the Russian Foundation for Basic Research–DFG, project no. 00-05040000, by the Russian Foundation for Basic Research, project no. 08–5-00600, and by the Federal Agency for Science and Innovations, projects nos. 43.700.11.00005, 43.043.11.1606, 01.700.12.0028.

REFERENCES

Allègre, C.J., Provost, A., and Jaupart, C., Oscillatory zoning: a pathological case of crystal growth, *Nature*, 1981, vol. 294, pp. 223–228.

Ariskin, A.A., Barmina, G.S., Frenkel, M.Ya., and Nielsen, R.L., COMAGMAT: a Fortran program to model magma differentiation processes, *Comput. Geosci.*, 1993, vol. 19, pp. 1155–1170.

Bindeman, I.N., Davis, A.M., and Drake, M.J., Ion microprobe study of plagioclase–basalt partition experiments at natural concentration level of trace elements, *Geochim. Cosmochim. Acta*, 1998, vol. 62, no. 7, p. 1175.

Brophy, J.G., Dorais, M.J., Donnelly-Nolan, J., and Singer, B.S., A textural and compositional (ion-probe and electron probe) study of plagioclase zonation styles in hornblende gabbro cumulates from Little Glass Mountain, Medicine Lake Volcano, California: implications for fractional crystallization mechanisms in calc-alkaline magma genesis, *Contrib. Mineral. Petrol.*, 1996, vol. 126, p. 121–136.

Browne, B.L., Eichelberger, J.C., Patino, L.C., et al., Magma mingling as indicated by texture and Sr/Ba ratios of plagioclase phenocrysts from Unzen Volcano, SW Japan, *J. Volcanol. Geothermal Res.*, 2006, vol. 154, pp. 103–116.

Browne, B., Izbekov, P., Eichelberger, J., and Churikova, T., Pre-eruptive storage conditions of the Holocene dacite erupted from Kizimen Volcano, Kamchatka, *International Geology Review*, 2010, vol. 52, no. 1, pp. 95–110.

Bunsen, R., Üeber die Prozesse der volkanischen Gesteinbildungen Islands, *Ann. Phys. Chem.,* 1851, no. 83, pp. 197–272.

Churikova, T., Dorendorf, F., and Wörner, G., Nature of geochemical zonality across Kamchatka island arc, in *Geodinamika i vulkanizm Kurilo-Kamchatskoi ostrovoduzhnoi sistemy* (Geodynamics and Volcanism of Kuril–Kamchatka Island Arc System), Petropavlovsk-Kamchatskii: Institute of Volcanology, Geology and Geochemistry, Far East Branch, RAS, 2001a, pp. 173–190.

Churikova, T., Wörner, G., Eichelberger, J. and Ivanov, B., Minor and trace element zoning in plagioclase from Kizimen Volcano, Kamchatka: insights on the magma chamber processes, in *Volcanism and Subduction: the Kamchatka Region*, Geophysical Monograph Series, vol. 172, Eichelberger, J. et al., Eds., Washington, DC: American Geophysical Union, 2007, pp. 303–324.

Churikova, T.G. and Sokolov, S.Yu., Magmatic evolution of Ploskie Sopki Volcano, Kamchatka: Analysis of strontium isotope geochemistry), *Geokhimiya*, 1993, no. 10, pp. 1439–1448.

Churikova, T. and Dorendorf, F., and Wörner, G., Sources and fluids in the mantle wedge below Kamchatka, evidence from across-arc geochemical variation, *J. Petrology*, 2001b, vol. 42, no. 8, pp. 1567–1593.

Churikova, T.G., Ivanov, B.V., Eichelberger, J., et al., Minor and trace elements in plagioclase—key to studying processes in magma chambers: Kizimen Volcano, Kamchatka, *Vulkanizm i geodinamika: materially II Vserossiiskogo simpoziuma po vulkanologii i paleovulkanologii* (Volcanism and Geodynamics: Materials of the Second All-Russia Symposium on Volcanology and Paleovolcanology), Yekaterinburg, 2003, pp. 446-451.

Couch, S., Sparks, R.S.J., and Carroll, M.R., Mineral disequilibrium in lavas explained by convective self-mixing in open magma chambers, *Nature*, 2001, vol. 411, pp. 1037–1039.

Davidson, J.P. and Tepley III, F.J., Recharge in volcanic systems: Evidence from isotope profiles of phenocrysts, *Science*, 1997, vol. 275, p. 826–829.

Dorendorf, F., Churikova, T., Koloskov, A., and Wörner, G., Late Pleistocene to Holocene activity at Bakening Volcano and surrounding monogenetic centers (Kamchatka): Volcanic geology and geochemical evolution, *J. of Volcanology and Geothermal Research*, 2000a, vol. 104, pp. 131–151.

Dorendorf, F., Wiechert, U., and Wörner, G., Hydrated sub-arc mantle: A source for the Kluchevskoy Volcano, Kamchatka, Russia, *Earth Planet. Sci. Lett.*, 2000b, vol. 175, pp. 69–86.

Dungan, M.A. and Rhodes, M.J., Residual glasses and melt inclusions in basalts from DSDP legs 45 and 46: Evidence for magma mixing, *Contrib. Mineral. Petrol.,* 1978, vol. 67, pp. 417–431.

Eichelberger, J.C., Andesitic volcanism and crustal evolution, *Nature*, 1978, vol. 275, pp. 21–27.

Eichelberger, J.C., Chertkoff, D.G., Dreher, S.T., and Nye, C.J., Magmas in collision: Rethinking chemical zonation in silicic magmas, *Geology*, 2000, vol. 28, no. 7, pp. 603–606.

Eichelberger, J.C., Izbekov, P.E., and Browne, B.L., Bulk chemical trends at arc volcanoes are not liquid lines of descent, *Lithos*, 2006, vol. 87, pp. 135–154.

Frikh-Khar, D.I., *Kristallizatsiya magmaticheskogo stekla i nekotorye voprosy petrogenezisa* (Crystallization of Magmatic Glass and Some Problems of Petrogenesis), Moscow: Nauka, 1977.

Ginibre, C., Kronz, A., and Wörner, G., High-resolution quantitative imaging of plagioclase composition using accumulated back-scattered electron images: New constraints on oscillatory zoning, *Contrib. Mineral. Petrol.*, 2002a, vol. 142, p. 436–448.

Ginibre, C., Wörner, G., and Kronz, A., Minor- and trace-element zoning in plagioclase: Implications for magma chamber processes at Parinacota Volcano, northern Chile, *Contrib. Mineral. Petrol.*, 2002b, vol. 143, pp. 300–315.

Grove, T.L., Baker, M.B., and Kinzler, R.J., Coupled CaAl–NaSi diffusion in plagioclase feldspar: Experiments and application to cooling rate speedometry, *Geochim. Cosmochim. Acta*, 1984, vol. 48, pp. 2113–2121.

Ivanov, B.V., Kadik, A.A., and Maksimov, A.P., Physicochemical conditions of crystallization of andesites of the Klyuchevskoi Volcanic Cluster, Kamchatka, *Geokhimiya*, 1978, no. 8, pp. 1139–1156.

Ivanov, B.V., *Andezity Kamchatki. Spravochnik khimicheskikh analizov vulkanitov i osnovnykh porodoobrazuyushchikh mineralov* (Andesites of Kamchatka. Reference Book of Chemical Analyses of Volcanic Rocks and Major Rock-Forming Minerals), Moscow: Nauka, 2008.

Kadik, A.A., Maksimov, A.P., and Ivanov, B.V., *Fiziko-khimicheskie usloviya kristallizatsii i genezis andezitov (na primere Klyuchevskoi gruppy vulkanov)* (Physicochemical Conditions of Crystallization and Genesis of Andesites: Klyuchevskoi Volcanic Cluster), Moscow: Nauka, 1986.

Kawamoto, T., Dusty and honeycomb plagioclase: Indicators of processes in the Uchino stratified magma chamber, Izu Peninsula, Japan, *J. Volcanol. Geotherm. Res.*, 1992, vol. 49, pp. 191–208.

Marsh, B.D., Magma chambers, *Ann. Rev. Earth Planet. Sci.*, 1989, vol. 17, pp. 439–474.

McNeill, A.W. and Danyushevsky, L.V., Composition and crystallization temperatures of primary melts from hole 896A basalts: Evidence from melt inclusion studies, *Proceedings of the Ocean Drilling Program. Scientific Results*, 1996, vol. 148, pp. 21–35.

Melekestsev, I.V., Ponomareva, V.V, and Volynets, O.N., Kizimen Volcano, Kamchatka: A future St. Helens?, *Vulkanol. Seismol.,* 1992, no. 4, pp. 8–32.

Naumov, V.B., Kovalenko, V.I., Babanskii, A.D., and Tolstykh, M.L., Genesis of andesites based on the data of studies of melt inclusions in minerals, *Petrologiya*, 1997, vol. 5, no. 6, pp. 654–665.

Plechov, P.Yu., Fomin, I.S., Mel'nik, O.E., and Gorokhova, N.V., Evolution of melt composition at intrusion of basalts into an acid magma chamber, *Vestnik MGU, Ser. IV, Geologiya,* 2008, no. 4, pp. 247–257.

Ponomareva, V.V., Churikova, T.G., Melekestsev, I.V., et al., Late Pleistocene–Holocene Volcanism of Kamchatka, in *Izmenenie okruzhayushchei sredy i klimata: prirodnye i svyazannye s nimi tekhnogennye katastrofy*, vol. 2, *Noveishii vulkanizm severnoi Evrazii: zakonomernosti razvitiya, vulkanicheskaya opasnost', svyaz' s glubinnymi protsessami i izmeneniyami prirodnoi sredy i klimata* (Changes of Environment and Climate: Natural and Associated Man-made Disasters, Neotectonic Volcanism of North Eurasia: Evolution Patterns, Volcanic Hazard, Relationships to Deep Processes and Changes of Environment and Climate), Laverov, N.P., et al., Eds., Moscow: IGEM RAN, IFZ RAN, 2008, pp. 19–40.

Sato, H., Mg-Fe partitioning between plagioclase and liquid in basalts of hole 504B, ODP leg 111: A study of melting at 1 atm, *Proceedings of the Ocean Drilling Program. Scientific Results*, 1989, vol. 111, p. 17–26.

Severs, M.J., Beard, J.S., Fedele, L., et al., Partitioning behavior of trace elements between dacitic melt and plagioclase, orthopyroxene, and clinopyroxene based on laser ablation ICPMS analysis of silicate melt inclusions, *Geochim. Cosmochim. Acta*, 2009, vol. 73, p. 2123–2141.

Stormer, J.C., The effects of recalculation on estimates of temperature and oxygen fugacity from analyses of multicomponent iron–titanium oxides, *American Mineralogist*, 1983, vol. 68, nos. 5–6, pp. 586–594.

Sun, S.-S. and McDonough W.F., Chemical and isotopic systematics of oceanic basalts: Implications for mantle composition and processes, in *Magmatism in the Ocean Basins*, Geological Society Special Publications, Saunders, A.D. and Norry, M.J., Eds., Geological Society of London, 1989, no. 42, pp. 313–345.

Tepley III, F.J., Davidson, J.P., Tilling, R.I., and Arth, J.G., Magma mixing, recharge and eruption histories recorded in plagioclase phenocrysts from El Chichón Volcano, Mexico, *J. Petrology,* 2000, vol. 41, no. 9, pp. 1397–1411.

Todt, W., Cliff, R.A., Hanser, A., and Hofmann, A.W., ^{202}Pb–^{205}Pb spike for Pb isotope analysis, *Terra Cognita*, 1984, vol. 4, pp. 209.

Tsuchiyama, A., Dissolution kinetics of plagioclase in the melt of the system diopside–albite–anorthite, and origin of dusty plagioclase in andesites, *Contrib. Mineral. Petrol.*, 1985, vol. 89, pp. 1–16.

Volynets, O.N., Popolitov, E.I., Flerov, G.B., and Kirsanov, I.T., Composition and geochemical characteristics of plagioclases from Quaternary volcanic rocks of Kamchatka and Kuril Islands, *Geokhimiya*, 1977, no. 5, pp. 736–747.

Volynets, O.N., Khrenov, A.P., Flerov, G.B., et al., On the place and time of crystallization of plagioclase phenocrysts in effusive rocks on the basis of studies of the products of present-day eruptions of volcanoes in the Kuril–Kamchatka zone, *Vulkanol. Seismol.*, 1979, no. 4, pp. 34–48.

Winter, J.D., *An Introduction to Igneous and Metamorphic Petrology*, New Jersey: Prentice-Hall Inc., 2001.

Translated by M. Isakin